Effect of Plastic Spin on Localization Predictions for a Porous Ductile Material

Tvergaard, Viggo; Giessen, Erik van der

Published in:
Journal of the Mechanics and Physics of Solids

DOI:
10.1016/0022-5096(91)90024-I

Publication date:
1991

J. Mech. Phys. Solids Vol. 39, No. 6, pp. 763–781, 1991.
Printed in Great Britain.

0022–5096/91 $3.00 + 0.00

EFFECT OF PLASTIC SPIN ON LOCALIZATION PREDICTIONS FOR A POROUS DUCTILE MATERIAL

VIGGO TVERGAARD† and ERIK VAN DER GIESSEN‡

† Department of Solid Mechanics, Technical University of Denmark, Lyngby, Denmark
‡ Laboratory for Engineering Mechanics, Delft University of Technology, Delft, The Netherlands

(*Received* 29 *January* 1990)

ABSTRACT

VARIOUS constitutive frameworks for macroscopic large strain elastoplasticity have recently identified the plastic spin as one of the key concepts in the description of anisotropic hardening. These theories involve a particular corotational stress rate that differs from the Jaumann stress rate by terms involving the plastic spin. This stress rate is introduced into a recently proposed material model for combined isotropic and kinematic hardening of a porous ductile solid. The plastic spin is taken to be governed by the simplest possible constitutive law, involving only one additional material parameter. An analysis of so-called unconstrained shearing is used to illustrate the effect of plastic spin on the stress response at large strains and finite material rotations. The effect of the plastic spin, via the corotational stress rate, on the predictions of strain localization in shear bands is studied in terms of simple model analyses. Results for various deformation and void nucleation conditions are discussed. The plastic spin is found to have a significant influence on the onset of localization even though the material rotations are still rather small at that instant. Also the progressive evolution of the shear band after localization until ductile fracture occurs in a void-sheet is strongly affected.

1. INTRODUCTION

INVESTIGATIONS of plastic flow localization in ductile materials show that predictions of the critical strain for localization are highly sensitive to details of the constitutive law (RICE, 1976). For the classical elastic–plastic solid with a smooth yield surface and normality of the plastic flow rule bifurcation into a shear band is not predicted at a realistic strain level, unless the material has essentially no strain hardening. However, formation of a vertex on the yield surface, plastic dilation (e.g. due to void growth), or non-normality of the plastic flow rule can significantly reduce the critical strain for flow localization (RUDNICKI and RICE, 1975; YAMAMOTO, 1978; NEEDLEMAN and RICE, 1978).

The analysis of localized necking in biaxially stretched thin sheets is the plane stress analogue of the shear band analysis (HILL, 1952) and shows similar sensitivity to the constitutive law (STÖREN and RICE, 1975). A kinematic hardening material model has been used by TVERGAARD (1978) to study sheet necking, and it was found that this model gives rise to more realistic localization strains. Bifurcation predictions for a perfect sheet are not affected by the assumption of kinematic hardening rather than isotropic hardening; but the imperfection-sensitivity is much increased by the higher

yield surface curvature at the point of loading. It was concluded (TVERGAARD, 1978) that the kinematic hardening model represents, in an approximate way, the effect of a smooth yield surface that develops a rounded vertex at the loading point.

Also predictions of shear band localization are strongly affected by the assumption of kinematic hardening, as has been found by HUTCHINSON and TVERGAARD (1981) in a study that focused primarily on solids that develop a sharp vertex on the yield surface. This was also found by MEAR and HUTCHINSON (1985) and TVERGAARD (1987), based on kinematic hardening versions of the porous ductile material model with isotropic hardening introduced by GURSON (1977a). In fact, the main motivation for suggesting these kinematic hardening material models was that the combined influence of porosity and the formation of a rounded vertex on the yield surface could be accounted for.

For a kinematic hardening solid subject to simple shear NAGTEGAAL and DE JONG (1982) found unrealistic oscillatory stress predictions at large strains. Many authors have subsequently investigated this problem, for a variety of different kinematic hardening laws, and it has been found (e.g. see DAFALIAS, 1983) that the stress oscillations disappear if certain corotational stress rates other than the Jaumann rate are used in the finite strain generalization of the constitutive law. In particular, following ideas of MANDEL (1971), some formulations decompose the continuum spin in an "elastic" part and a plastic part and use corotational stress rates based on the "elastic" part of the spin (e.g. DAFALIAS, 1983, 1985; LORET, 1983). Then, constitutive laws must be assumed for the plastic spin, and it turns out that the result, whether or not stress oscillations are predicted at large shear strains, is quite sensitive to these assumptions.

For biaxially stretched thin sheets the principal stress and strain directions remain fixed during necking, so that spinning of the material does not play a role. Therefore, the strong effect of kinematic hardening on predictions of localization in thin sheets found by TVERGAARD (1978) is not affected by assumptions regarding plastic spin. On the other hand, predictions of localization in shear bands are affected by the way in which plastic spin is incorporated in the constitutive law. Usually, the shear strains and the spin are quite small at the onset of localization: but during the subsequent localized plastic flow inside the band shear strains certainly may grow large enough to cause unrealistic stress oscillations analogous to those found by NAGTEGAAL and DE JONG (1982).

In the present paper alternative versions of the kinematic hardening ductile porous material model of MEAR and HUTCHINSON (1985) and TVERGAARD (1987) are introduced by using different corotational stress rates based on different parameters in a simple constitutive law for the plastic spin. The material models are used to predict the onset of localization as well as the post-localization behaviour leading to ductile fracture in a void-sheet, and the predictions of different models are compared.

2. COROTATIONAL STRESS RATES

Following the findings of NAGTEGAAL and DE JONG (1982), many alternative stress rates have been considered to replace the Jaumann rate. The particular stress rate we

consider here, follows from a class of elastoplasticity theories for large deformations of anisotropic solids as formulated first by MANDEL (1971) and adopted by several others later. In this theory, the kinematics of the continuum and the kinematics of the underlying material substructure which determines the current anisotropy are treated as distinct entities. In addition to the usual additive decomposition of the strain-rate $\mathbf{d}$ into elastic and plastic parts $\mathbf{d}^E$ and $\mathbf{d}^P$, respectively, this leads to a similar decomposition of the continuum spin $\boldsymbol{\omega}$

$$\mathbf{d} = \mathbf{d}^E + \mathbf{d}^P, \quad \boldsymbol{\omega} = \boldsymbol{\omega}^E + \boldsymbol{\omega}^P. \tag{2.1}$$

Here, the "elastic" part $\boldsymbol{\omega}^E$ is the spin of the substructure, and the plastic spin $\boldsymbol{\omega}^P$ represents the spin of the material relative to the underlying substructure.

Furthermore, these theories show that the evolution laws of tensorial structure variables must be expressed in terms of rates which involve corotation with the substructural spin rather than with the continuum spin. In particular, the evolution law of the back stress tensor $\boldsymbol{\alpha}$ in a kinematic hardening model is expressed in terms of the stress rate $\overset{\circ}{\boldsymbol{\alpha}}$ defined by

$$\overset{\circ}{\boldsymbol{\alpha}} = \dot{\boldsymbol{\alpha}} - \boldsymbol{\omega}^E \cdot \boldsymbol{\alpha} + \boldsymbol{\alpha} \cdot \boldsymbol{\omega}^E \tag{2.2}$$

if we confine attention to small elastic strains (see e.g. DAFALIAS, 1983, 1985; LORET, 1983). This rate is related to the usual Jaumann rate, indicated by a superposed ∇, according to

$$\overset{\nabla}{\boldsymbol{\alpha}} = \overset{\circ}{\boldsymbol{\alpha}} - \boldsymbol{\omega}^P \cdot \boldsymbol{\alpha} + \boldsymbol{\alpha} \cdot \boldsymbol{\omega}^P \tag{2.3}$$

in terms of the plastic spin $\boldsymbol{\omega}^P$.

In addition to the constitutive equations for the plastic strain-rate it is here necessary to assume constitutive relations for the plastic spin. In this section we will discuss a few simple models for homogeneous void-free solids that are initially isotropic. These will serve as a reference for the development of the porous material model in the next section. First we note that general invariance requirements may be used to show that the plastic spin in an isotropic hardening model must vanish identically (see e.g. MANDEL, 1971) so that the stress rate $(^{\circ})$ reduces to the Jaumann rate. For a J_2 type kinematic hardening model where the plastic strain-rate $\mathbf{d}^P$ is proportional to the deviator of $(\boldsymbol{\sigma} - \boldsymbol{\alpha})$, with $\boldsymbol{\sigma}$ denoting the Cauchy stress, DAFALIAS (1983, 1985) and LORET (1983) independently proposed the following expression for the plastic spin

$$\boldsymbol{\omega}^P = \tfrac{1}{2}\rho(\boldsymbol{\alpha} \cdot \mathbf{d}^P - \mathbf{d}^P \cdot \boldsymbol{\alpha}) \tag{2.4}$$

which was subsequently used by several others. According to this expression, the plastic spin vanishes in states where the tensors $\boldsymbol{\alpha}$ and $\mathbf{d}^P$ are coaxial. The evolution of the back stress is taken to be given by the finite strain generalization

$$\overset{\circ}{\boldsymbol{\alpha}} = \dot{\mu}(\boldsymbol{\sigma} - \boldsymbol{\alpha}) \tag{2.5}$$

of ZIEGLER's (1959) hardening rule in terms of the stress rate defined in (2.2).

The factor ρ in the expression (2.4) appears as an additional material function in this kinematic hardening model which would have to be determined from experiments; but the information available on this in the literature is very limited. For simplicity, DAFALIAS (1983, 1985) and LORET (1983) considered constant values of ρ normalized

by the initial yield stress σ_y. On the basis of an analysis of the spin during simple shear of a material element which may be associated with an induced preferred orientation, PAULUN and PECHERSKI (1987) proposed to specify ρ by the function

$$\rho = \sqrt{\frac{3}{2}\frac{12\alpha_e}{h_\gamma^2 + 3\alpha_e^2}} \tag{2.6}$$

in terms of $\alpha_e = (3\mathbf{a}\cdot\mathbf{a}/2)^{1/2}$ and the hardening factor $h_\gamma = EE_t/(E-E_t)$, where E and E_t are Young's modulus and the tangent modulus, respectively, and $\mathbf{a}$ is the deviator of $\boldsymbol{\alpha}$.

The elastic stress strain relationship used here can be cast in rate form for small elastic strains as (see e.g. LORET, 1983)

$$\boldsymbol{\sigma} = \mathbf{R} : \mathbf{d}^E \tag{2.7}$$

in terms of the stress rate

$$\boldsymbol{\sigma} = \dot{\boldsymbol{\sigma}} - \boldsymbol{\omega}^P\cdot\boldsymbol{\sigma} + \boldsymbol{\sigma}\cdot\boldsymbol{\omega}^P \tag{2.8}$$

and where, as usual

$$R^{ijkl} = \frac{E}{1+\nu}\left\{\frac{1}{2}(G^{ik}G^{jl} + G^{il}G^{jk}) + \frac{\nu}{1-2\nu}G^{ij}G^{kl}\right\} \tag{2.9}$$

with E and ν being Young's modulus and Poisson's ratio. Here and in the sequel, components are taken with respect to the current deformed base vectors $\mathbf{G}_i$ of the convected coordinated system x^i; e.g. $\boldsymbol{\sigma} = \sigma^{ij}\mathbf{G}_i\mathbf{G}_j$, $\boldsymbol{\omega}^P = \omega_{ij}^P\mathbf{G}^i\mathbf{G}^j$ and $\mathbf{d} = \dot{\eta}_{ij}\mathbf{G}^i\mathbf{G}^j$ with pertinent superscripts E or P. The metric tensors in the current configuration and the reference configuration are denoted by G_{ij} and g_{ij}, respectively.

Written in terms of components on the current base vectors the expressions (2.3) and (2.4) take the form

$$\overset{\nabla}{\alpha}{}^{ij} = \boldsymbol{\alpha}^{ij} - (G^{ik}\alpha^{jl} - \alpha^{ik}G^{jl})\omega_{kl}^P, \tag{2.10}$$

$$\omega_{ij}^P = \tfrac{1}{2}\rho(G_{ik}\dot{\eta}_{jl}^P - \dot{\eta}_{ik}^P G_{lj})\alpha^{kl}. \tag{2.11}$$

The difference of the kinematic hardening model thus obtained with the finite strain generalization introduced by TVERGAARD (1978) lies only in the appearance of the corotational rate $\overset{\nabla}{(\ )}$ in (2.5) and (2.7) instead of the Jaumann rate. The expression (2.4) for the plastic spin used here is among the simplest of the various constitutive relations that have been proposed in recent years on the basis of tensor representation theorems. A completely different development which assumes a non-symmetric back stress is discussed by VAN DER GIESSEN (1989, 1990). The adequacy of the recent plastic spin proposals for arbitrary loading paths and various anisotropies is currently under investigation.

3. Porous Ductile Material

Many studies of ductile fracture mechanisms have been based on the isotropic hardening constitutive relations proposed by Gurson (1977a, b). A kinematic hardening version of this material model was suggested by Mear and Hutchinson (1985) for a porous ductile solid, and Tvergaard (1987) extended the model to account for void nucleation.

The model makes use of a family of isotropic/kinematic hardening yield surfaces of the form $\Phi(\sigma^{ij}, \alpha^{ij}, \sigma_F, f) = 0$, where f is the current void volume fraction, σ^{ij} is the average macroscopic Cauchy stress tensor and α^{ij} denotes the stress components at the centre of the yield surface. The radius σ_F of the yield surface for the matrix material is taken to be given by

$$\sigma_F = (1-b)\sigma_y + b\sigma_M, \tag{3.1}$$

where σ_y and σ_M are the initial yield stress and the matrix flow stress, respectively, and the parameter b is a constant in the range $[0, 1]$. The constitutive relations are formulated such that for $b = 1$ they reduce to Gurson's (1977a) isotropic hardening model, whereas a pure kinematic hardening model appears for $b = 0$.

The approximate yield condition for a porous solid to be used here is of the form

$$\Phi = \frac{\tilde{\sigma}_e^2}{\sigma_F^2} + 2q_1 f^* \cosh\left[\frac{\tilde{\sigma}_k^k}{2\sigma_F}\right] - 1 - (q_1 f^*)^2 = 0, \tag{3.2}$$

where $\tilde{\sigma}^{ij} = \sigma^{ij} - \alpha^{ij}$, $\tilde{\sigma}_e = (3\tilde{s}_{ij}\tilde{s}^{ij}/2)^{1/2}$ and $\tilde{s}^{ij} = \tilde{\sigma}^{ij} - G^{ij}\tilde{\sigma}_k^k/3$. For $f^* = f$ and $q_1 = 1$ the expression (3.2) is that proposed by Mear and Hutchinson (1985), which coincides with that of Gurson (1977a) for $b = 1$. The parameter $q_1 > 1$ has been proposed to bring predictions of the Gurson model at low void volume fractions in better agreement with full numerical analyses for periodic arrays of voids (Tvergaard, 1981, 1982a). The function $f^*(f)$ was introduced to model the more rapid loss of material stress carrying capacity during final failure by void coalescence (Tvergaard and Needleman, 1984)

$$f^*(f) = \begin{cases} f, & \text{for } f \leqslant f_C, \\ f_C - \dfrac{f_U^* - f_C}{f_F - f_C}(f - f_C), & \text{for } f > f_C. \end{cases} \tag{3.3}$$

The modification (3.3) of the function (3.2) becomes active when f exceeds a certain critical value f_C, and final fracture occurs for $f = f_F$ [i.e. $f^*(f_F) = f_U^* = 1/q_1$]. The values $f_C = 0.15$ and $f_F = 0.25$ were originally proposed, based on experimental results and numerical model analyses, but more recent investigations indicate that smaller values of f_C may be more realistic (e.g. see Tvergaard, 1990b).

The plastic part of the macroscopic strain increment $\dot{\eta}_{ij}^p$ and the effective plastic strain increment $\dot{\varepsilon}_M^p$ for the matrix material are taken to be related by (Tvergaard, 1987)

$$\tilde{\sigma}^{ij}\dot{\eta}_{ij}^p = (1-f)\sigma_F \dot{\varepsilon}_M^p. \tag{3.4}$$

For $f = 0$ (3.4) is an exact relationship for the classical kinematic hardening solid,

and for $h = 1$ (3.4) reduces to the equivalent plastic work expression applied by GURSON (1977a). If the increments of the matrix plastic strain and the matrix flow stress are taken to be related by the uniaxial true stress natural strain curve for the matrix material $\dot{\varepsilon}_M^p = (1/E_t - 1/E)\dot{\sigma}_M$, (3.4) gives

$$\dot{\sigma}_M = \frac{EE_t}{E - E_t} \frac{\tilde{\sigma}^{ij}\dot{\eta}_{ij}^p}{(1-f)\sigma_F}. \tag{3.5}$$

The change of the void volume fraction during an increment of deformation is taken to be given by

$$\dot{f} = (1-f)G^{ij}\dot{\eta}_{ij}^p + \mathscr{A}\dot{\sigma}_M + \mathscr{B}(\dot{\sigma}_k^k)/3, \tag{3.6}$$

where the first term results from the growth of existing voids, and the two last terms model the increment due to nucleation (NEEDLEMAN and RICE, 1978). Nucleation controlled by the plastic strain ε_M^p is represented by taking $\mathscr{A} > 0$ and $\mathscr{B} = 0$ in (3.6), and nucleation is assumed to follow a normal distribution, with the mean nucleation strain ε_N, the standard deviation s and the volume fraction f_N of void nucleating particles (TVERGAARD, 1987). If nucleation is controlled by the maximum normal stress on the particle–matrix interface, the sum $\sigma_M + \sigma_k^k/3$ is used as an approximate measure of this maximum stress, thus taking $\mathscr{A} = \mathscr{B}$.

A fictitious Gurson yield surface $\Phi_G = \Phi_G(\sigma_G^{ij}, \sigma_M, f)$ was used by TVERGAARD (1987) to formulate the constitutive relations, where σ_M and f are the current values, and σ_G^{ij} are a set of fictitious stress components chosen such that

$$\frac{\sigma_G^{ij}}{\sigma_M} = \frac{\tilde{\sigma}^{ij}}{\sigma_F}. \tag{3.7}$$

With this assumption, $\Phi_G = 0$ is a direct consequence of $\Phi = 0$. In most cases the fictitious stresses σ_G^{ij} will differ from the actual stresses σ^{ij} at every point of the current yield surface.

The expression for $\dot{\eta}_{ij}^p$ in a point of the yield surface $\Phi = 0$ is chosen identical to that given by the Gurson model at the point σ_G^{ij} of the fictitious surface $\Phi_G = 0$. In the present paper the plastic part of the strain rate is taken to be given in terms of the alternative stress rate σ^{kl} (2.8). Thus, the expression is here taken to be

$$\dot{\eta}_{ij}^p = \frac{1}{H} m_{ij}^G m_{kl}^F \sigma^{kl}, \tag{3.8}$$

where

$$m_{ij}^G = \frac{3}{2}\frac{\tilde{s}_{ij}}{\sigma_F} + \alpha G_{ij}, \qquad m_{ij}^F = \frac{3}{2}\frac{\tilde{s}_{ij}}{\sigma_F} + \beta G_{ij}, \tag{3.9}$$

$$\alpha = \frac{f^*}{2} q_1 \sinh\left(\frac{\tilde{\sigma}_k^k}{2\sigma_F}\right), \qquad \beta = \alpha + \frac{\mathscr{B}\sigma_M}{6}\frac{\partial\Phi}{\partial f}, \tag{3.10}$$

$$H = \frac{\sigma_M}{2}\left[-3\alpha(1-f)\frac{\partial\Phi}{\partial f} - \left\{\frac{\partial\Phi}{\partial f}\mathscr{A} + \frac{\sigma_F}{\sigma_M}\frac{\partial\Phi}{\partial\sigma_F}\right\}\frac{EE_t}{E-E_t}\frac{1}{1-f}\left(\frac{\tilde{\sigma}_e^2}{\sigma_F^2} + \alpha\frac{\tilde{\sigma}_k^k}{\sigma_F}\right)\right]. \tag{3.11}$$

Plastic yielding initiates when $\Phi = 0$ and $\dot{\Phi} > 0$ during elastic deformation, and continued plastic loading requires $\Phi = 0$ and $(1/H)m^F_{kl}\overset{\circ}{\sigma}{}^{kl} \geqslant 0$. Note that m^F_{ij} deviates from the normal m^G_{ij} of the surface $\Phi = 0$ when $\mathscr{B} \neq 0$.

The finite strain generalization of ZIEGLER's (1959) hardening rule, expressing the evolution of the yield surface centre during a plastic increment, is here chosen as in (2.5), i.e.

$$\overset{\circ}{\alpha}{}^{kl} = \dot{\mu}\tilde{\sigma}^{kl}, \qquad \dot{\mu} \geqslant 0. \tag{3.12}$$

Using the identities $\tilde{s}_{kl}(\overset{\nabla}{\sigma}{}^{kl} - \overset{\nabla}{\alpha}{}^{kl}) = \tilde{s}_{kl}(\overset{\circ}{\sigma}{}^{kl} - \overset{\circ}{\sigma}{}^{kl})$, $G_{kl}(\overset{\nabla}{\sigma}{}^{kl} - \overset{\nabla}{\alpha}{}^{kl}) = G_{kl}(\overset{\circ}{\sigma}{}^{kl} - \overset{\circ}{\sigma}{}^{kl})$ and $G_{kl}\overset{\nabla}{\sigma}{}^{kl} \equiv G_{kl}\overset{\circ}{\alpha}{}^{kl}$ the value of the parameter $\dot{\mu}$ is determined so that the consistency condition, $\dot{\Phi} = 0$, is satisfied:

$$\dot{\mu} = (1-b)\frac{1}{2}\left[\frac{\tilde{\sigma}^2_e}{\sigma^2_F} + \alpha\frac{\tilde{\sigma}^k_k}{\sigma_F}\right]^{-1}\left[\frac{2}{\sigma_F}m^G_{kl}\overset{\circ}{\sigma}{}^{kl} + \frac{\sigma_y}{\sigma_F}\frac{\partial\Phi}{\partial f}\frac{\mathscr{B}}{3}G_{kl}\overset{\circ}{\sigma}{}^{kl}\right.$$

$$\left. + \frac{\sigma_y}{\sigma_F}\frac{1}{H}\frac{\partial\Phi}{\partial f}\left\{3\alpha(1-f) + \mathscr{A}\frac{EE_t}{E-E_t}\frac{1}{1-f}\left[\frac{\tilde{\sigma}^2_e}{\sigma^2_F} + \alpha\frac{\tilde{\sigma}^k_k}{\sigma_F}\right]\right\}m^F_{kl}\overset{\circ}{\sigma}{}^{kl}\right]. \tag{3.13}$$

It is noted that in the analogous expression for $\dot{\mu}$ in (TVERGAARD, 1987) one term was wrong in the case of stress controlled nucleation (as also stated by TVERGAARD, 1990a). The results were correct though, since $\dot{\mu}$ was corrected numerically in each increment to exactly satisfy $\Phi = 0$.

Now, using the elastic incremental stress strain relationship (2.7), the following expression for the Kirchhoff stress increment in terms of the total Lagrangian strain increment is derived

$$\dot{\tau}^{ij} = \mathscr{L}^{ijkl}\dot{\eta}_{kl} - \delta\hat{M}^{ij}_G M^{kl}_F\dot{\eta}_{kl}, \tag{3.14}$$

where

$$M^{ij}_G = \mathscr{R}^{ijkl}m^G_{kl}, \qquad M^{kl}_F = m^F_{rs}\mathscr{R}^{rskl}, \tag{3.15}$$

$$\delta = \begin{cases} 0, & \text{for elastic unloading} \\ \sqrt{(G/g)}\,[H + m^F_{rs}\mathscr{R}^{rskl}m^G_{kl}]^{-1}, & \text{for plastic loading,} \end{cases} \tag{3.16}$$

$$\hat{M}^{ij}_G = M^{ij}_G + (G^{ir}\sigma^{js} - \sigma^{ir}G^{js})\Omega_{rs},$$

$$\Omega_{rs} = \frac{\rho}{2}(G_{rk}m^G_{ls} - m^G_{rk}G_{ls})\alpha^{kl}, \tag{3.17}$$

$$\mathscr{L}^{ijkl} = \sqrt{(G/g)}\,[\mathscr{R}^{ijkl} - \tfrac{1}{2}(\sigma^{ik}G^{jl} + \sigma^{jk}G^{il} + \sigma^{il}G^{jk} + \sigma^{jl}G^{ik}) + \sigma^{ij}G^{kl}]. \tag{3.18}$$

Apart from the terms in (3.17), resulting from the plastic spin, (3.14)–(3.18) are analogous to expressions given by TVERGAARD (1982c).

The uniaxial true stress logarithmic strain curve for the matrix material is taken to be presented by the piecewise power law

$$\varepsilon = \begin{cases} \dfrac{\sigma}{E}, & \text{for } \sigma \leqslant \sigma_Y \\ \dfrac{\sigma_Y}{E}\left(\dfrac{\sigma}{\sigma_Y}\right)^n, & \text{for } \sigma > \sigma_Y, \end{cases} \tag{3.19}$$

where E is Young's modulus, and n is the strain hardening exponent.

4. Behaviour in Shear

In this section we briefly study the effect of plastic spin on the response of void-free material subject to so-called unconstrained shearing. This is a plane homogeneous deformation process where a block of material is deformed in simple shear in the x_1, x_2 plane, under plane strain conditions in the x_3-direction, while simultaneous extension in the x_2-direction is allowed to release the normal stress in that direction. Using components on fixed Cartesian coordinates, the process is characterized by components $L_{12} = \dot{\gamma}/e$, $L_{22} = \dot{e}/e$, $L_{ij} = 0$ otherwise, of the velocity gradient $\mathbf{L} = \mathbf{d} + \boldsymbol{\omega}$, such that $\sigma_{22} = \sigma_{i3} = 0$ ($i, j = 1, \ldots, 3$) and where γ is the shear strain and e the extensional stretch. This process approximates the conditions inside a shear band oriented at $\psi = 45°$ (see Fig. 3) in an otherwise elastic material subject to a stress state $\sigma_2^0 = -\sigma_1^0$ (see Section 5).

To illustrate the effect of plastic spin, we focus on homogeneous void-free materials assuming either isotropic ($h = 1$) or kinematic hardening ($h = 0$). The constitutive equations can be obtained from (3.8), (3.18) by substituting $f = f^* = 0$. Just as in the localization analyses to be presented in Section 5, the materials are specified by $\sigma_Y/E = 0.0033$, $\nu = 0.3$ and $n = 10$. The effect of plastic spin is studied by considering three different plastic spin parameters ρ in (2.4) or (3.17): either ρ is constant and takes values $\rho = 0$ or $\rho = 2/\sigma_Y$, or ρ is taken to be given by the expression (2.6).

Figure 1 shows the development of the shear stress σ_{12} during unconstrained shearing as a function of the maximum principal logarithmic strain ε_1 up to strains of about 2.5 ($\gamma \approx 10$). As mentioned before, the kinematic hardening model ($h = 0$) with $\rho = 0$ reduces to the classical J_2 kinematic hardening model (TVERGAARD, 1978) and it is seen that it predicts an oscillatory stress response for large strains, like that observed by NAGTEGAAL and DE JONG (1982) in simple shear. We recall that this behaviour was recognized by LORET (1983), DAFALIAS (1983, 1985) and others to be an artifact of the use of the Jaumann rate. For increasing values of ρ, hence for an increasing contribution of the plastic spin, the oscillatory behaviour is seen to fade out. For $\rho = 2/\sigma_Y$, the shear stress reaches a maximum at $\varepsilon_1 = 0.39$ shortly after the first peak in the response for $\rho = 0$, but then remains a monotonic function of ε_1 up to $\varepsilon_1 \approx 2.5$. For large values of ρ, for instance $\rho = 5/\sigma_Y$, the stress response is completely monotonic, just like that for isotropic hardening ($h = 1$). Note that these results differ considerably from those obtained for simple shear by DAFALIAS (1985), where a monotonic response is found already with $\rho < 1/\sigma_Y$ using linear hardening ($E_t =$ const.). This shows that the oscillatory behaviour is not determined solely by the plastic spin parameter, but also by the hardening characteristics. The expression

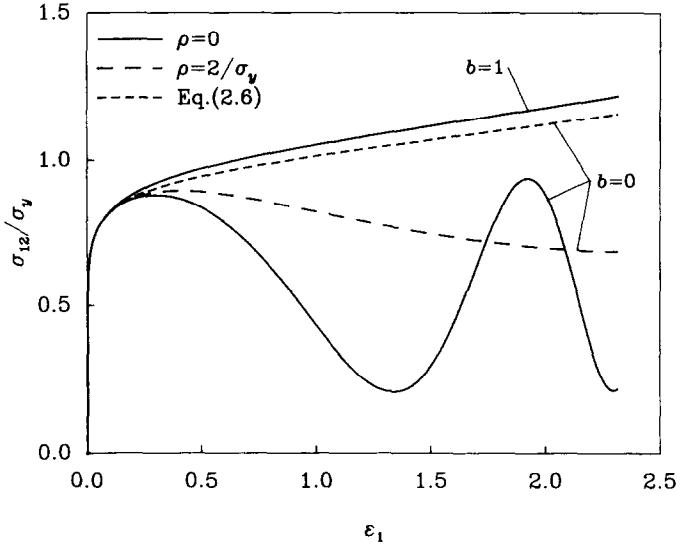

FIG. 1. Shear stress vs maximum principal logarithmic strain during unconstrained shearing of void-free material.

(2.6) for ρ indeed depends directly on the hardening of the material. The shear stress response is seen to be completely monotonic and, in fact, rather close to the prediction of the isotropic hardening model.

The normal stress σ_{11} in the shearing direction that accompanies the deformation process is very small ($\sigma_{11}/\sigma_y < 0.03$) for isotropic hardening ($b = 1$), while it oscillates for the classical kinematic hardening model ($b = 0$, $\rho = 0$), reaching a first maximum of $\sigma_{11}/\sigma_y \approx 0.8$ at $\varepsilon_1 \approx 0.9$. For $\rho = 2/\sigma_y$, σ_{11} increases monotonically with ε_1 and tends to saturate at a value of about σ_y. For increasing ρ this behaviour is essentially maintained but the asymptotic value decreases. For ρ according to (2.6) the maximum value of σ_{11} is about half that for $\rho = 2/\sigma_y$.

Thus it is observed that a rather broad variety of stress responses during large strains may result from different values of the plastic spin parameter ρ. For shearing up to a principal strain $\varepsilon_1 \approx 0.25$ the stress responses for kinematic hardening with different ρ seem to be rather close. However, it should also be observed that for strains below this value, the particular value of ρ does have a noticeable effect on the slopes of the σ_{12}–ε_1 and σ_{11}–ε_1 curves and thus on the stress increment directions in stress space. This is illustrated in Fig. 2 where the stress increments $d\sigma_{ij}/d\varepsilon_1$ at $\varepsilon_1 = 0.125$ are plotted in σ_{11}–σ_{12} space. It is seen that the stressing directions in kinematic hardening deviate considerably from that in isotropic hardening, and furthermore that there is a noticeable effect of the plastic spin, already at this somewhat smaller strain. For increasing values of the plastic spin parameter ρ, the stress increment direction is shifted somewhat in the direction of that corresponding to isotropic hardening. This seems to indicate a reduction of the effect of the yield surface curvature with increasing ρ.

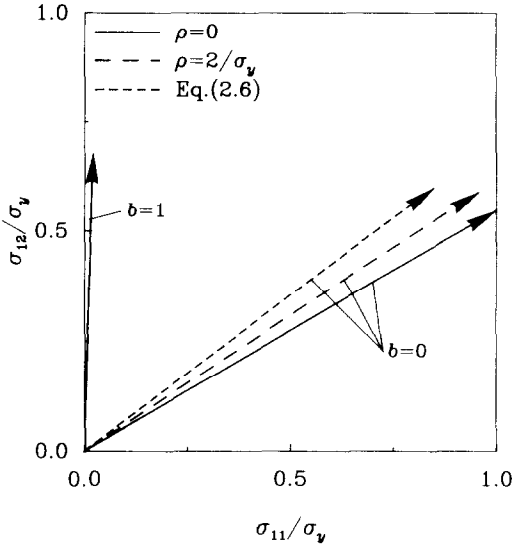

FIG. 2. Stress increments $d\sigma_{ij}/d\varepsilon_I$ in σ_{11}, σ_{12} space at $\varepsilon_I = 0.125$ during unconstrained shearing of void-free material.

5. SHEAR BANDS IN PLANE STRAIN OR AXISYMMETRIC TENSION

Simple model studies for the onset of plastic flow localization were used by MEAR and HUTCHINSON (1985) and TVERGAARD (1987) to illustrate the effect of incorporating kinematic hardening in the constitutive relations for a ductile porous material. The same type of analyses are carried out here to study the different constitutive laws obtained by using different corotational stress rates in the finite strain generalization of kinematic hardening. Furthermore, the present computations are continued beyond the onset of localization, to study the effect of the constitutive descriptions on the prediction of void-sheet fracture inside the shear band.

The model analyses assume an initial material inhomogeneity, such as a higher concentration of void nucleating particles or a lower initial yield stress inside a plane slice of material, and the stress-states inside and outside this slice of material, respectively, are assumed to remain homogeneous throughout the deformation history. A Cartesian x^i-coordinate system in the initial state is used as reference, and the principal directions outside the band are assumed to remain fixed, parallel with the x^i-direction (see Fig. 3), and the slice of material containing the initial inhomogeneity is

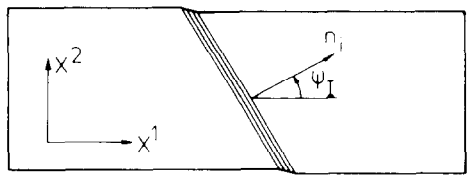

FIG. 3. Plastic flow localization in a uniformly strained solid.

assumed parallel with the x^3-axis, with the initial angle of inclination ψ_I and the unit normal vector n_i. In the following superscript b and zero denote quantities inside and outside the band, respectively.

The uniform state outside the band is specified by the following fixed ratios of principal logarithmic strains ε_i and principal true stresses σ_i

$$\varepsilon_3^0 = \xi\varepsilon_2^0, \qquad \sigma_2^0 = \kappa\sigma_1^0, \tag{5.1}$$

while ε_1^0 increases monotonically up to the onset of localization. Plane strain conditions are specified by $\xi = 0$, while $\xi = 1$ gives axisymmetric conditions outside the band. Uniaxial plane strain tension or uniaxial tension are specified by taking $\kappa = 0$, while larger values of κ can be used to study the effect of a superposed hydrostatic tension. In terms of the principal strains outside the band and the initial angle of inclination ψ_I of the band the current angle of inclination ψ is given by

$$\tan\psi = \exp(\varepsilon_1^0 - \varepsilon_2^0)\tan\psi_I. \tag{5.2}$$

Compatibility requires no jump in tangential derivatives of the displacement components u_i over the band interface. Thus the displacement gradients inside the band can be expressed in terms of those outside as

$$u_{i,j}^b = u_{i,j}^0 + c_i n_j, \tag{5.3}$$

where c_i are parameters to be determined. Equilibrium requires continuity of nominal tractions T^i over the band interface

$$(T^i)^b = (T^i)^0, \tag{5.4}$$

where the tractions on a surface with reference normal n_j are given by $T^i = (\tau^{ij} + \tau^{kj}u_k^i)n_j$. Now, for a prescribed stress or strain history outside the band, a set of incremental equations for $\dot{c}_i$ are obtained by substituting the constitutive relations and the incremental form of (5.3) into the incremental form of (5.4).

If there is no material inhomogeneity, the incremental equations for $\dot{c}_i$ are homogeneous. The first possibility of a non-trivial solution occurs at a bifurcation point, which marks the loss of ellipticity of the governing field equations. For proportional stressing histories the instantaneous moduli corresponding to the present kinematic hardening models ($b < 1$) remain identical to those for isotropic hardening ($b = 1$), independent of plastic spin, since the principal directions remain fixed. Therefore, the effect of kinematic hardening on localization predictions is tied to the presence of initial imperfections (see also TVERGAARD, 1978).

It is noted that the present shear band model reduces to the conditions of unconstrained shearing analysed in Section 4, if $\psi_I = 45^\circ$, $\kappa = -1$ and $\xi = 0$, while deformations outside the band are neglected. Such analyses for the shear band model, with only elastic deformations outside the band, have shown good agreement with the results presented in Fig. 1.

In the cases to be analysed here the materials are taken to be power hardening, with $\sigma_y/E = 0.0033$, $n = 10$, Poisson's ratio $\nu = 0.3$, $q_1 = 1.5$, and $f_C = 0.15$, $f_F = 0.25$ in (3.3). The initial void volume fraction is taken to be zero in all cases, $f_I^0 = f_I^b = 0$, and the volume fraction of void nucleating particles is taken to be larger inside the band,

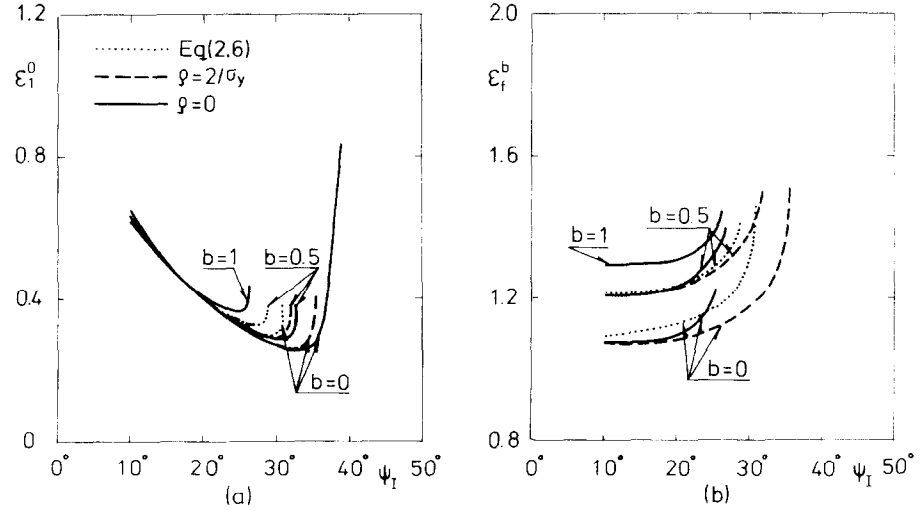

FIG. 4. Uniaxial plane strain tension, $\xi = \kappa = 0$, and strain controlled nucleation, $\Delta f_N = 0.01$, $f_N^0 = 0$, $\varepsilon_N = 0.3$, $s = 0.1$. (a) Localization strain vs initial band orientation. (b) Fracture strain vs initial band orientation.

$$f_N^0 = f_N^0 + \Delta f_N, \tag{5.5}$$

so that the initial imperfection is specified by Δf_N. Nucleation is taken to be strain controlled with the standard deviation $s = 0.1$ and with the mean nucleation strain $\varepsilon_N = 0.3$ in the first cases analysed.

The results in Fig. 4 are obtained for uniaxial plane strain tension [$\xi = \kappa = 0$ in (5.1)] in a case where voids nucleate only inside the band, $f_N^0 = 0$, $\Delta f_N = 0.01$. Three different corotational stress rates (2.8) are used in these analyses, one based on taking $\rho = 0$ in (2.4), thus using the Jaumann rate, one based on $\rho = 2/\sigma_y$, and one based on the expression (2.6) for ρ as suggested by PAULUN and PECHERSKI (1987). The value $\rho = 2/\sigma_y$ is the smallest constant value for which the oscillatory behaviour of the stresses disappears in the pure shear analyses of Fig. 1. Thus, the constitutive description obtained for $\rho = 2/\sigma_y$ assumes just enough plastic spin so that the predicted material behaviour is also reasonable in the range of large shearing. According to Fig. 1 the expression (2.6) for ρ gives more conservative predictions of kinematic hardening, comparable to taking constant values of $5/\sigma_y$ to $10/\sigma_y$. It is noted that these different corotational stress rates coincide for isotropic hardening, so that all predictions of localization and post-localization behaviour are identical for $h = 1$.

Due to the material inhomogeneity the strains grow larger inside the band than outside once nucleation starts to occur, and localization is defined by the onset of elastic unloading outside the band. For each of the curves plotted in Fig. 4a the minimum identifies the most critical initial angle of inclination of the band containing the inhomogeneity. For pure kinematic hardening, $h = 0$, Fig. 4a shows clear differences between the localization predictions of the different constitutive models considered here. The minimum localization strain found for $\rho = 2/\sigma_y$ is only slightly

higher than that for $\rho = 0$, but the curve for ρ according to (2.6) shows noticeably later localization. For mixed kinematic and isotropic hardening ($b = 0.5$) the same trends are found, with localization predictions between those for $b = 0$ and $b = 1$. It is noted that also LORET (1985) has found that the plastic spin delays the onset of localization.

After the onset of localization shear deformations continue inside the band, while the longitudinal strain ε_1^0 outside the band decays slowly as the tensile stress decays. The high localized deformations, leading to failure inside the band, add little to the overall deformations of the solid, and therefore the strain outside the band at the onset of localization is a relevant failure value. However, the computations can be continued to study the growth of voids inside the band, until failure occurs by coalescence in a so-called void-sheet. Such analyses have been carried out by TVERGAARD (1982b) for an isotropic hardening solid ($b = 1$) subject to various stress states.

In the present paper all localization analyses have been continued beyond the onset of elastic unloading outside the band. With the chosen parameter values in (3.3) the stress starts to decay very rapidly when the void volume fraction f reaches the value 0.15, and total loss of stress carrying capacity occurs at 0.25. The fracture strain ε_f^b plotted in Fig. 4b denotes the value of the maximum principal logarithmic strain inside the band, at the stage where the void volume fraction reaches the value $f^b = 0.20$ (a little before final failure).

For isotropic hardening ($b = 1$) the void volume fraction inside the band grows continuously in the post-localization range, reaching the value $f = 0.20$ at a strain ε_f^b in the range from 1.29 to 1.44, as shown in Fig. 4b. However, for kinematic hardening with $\rho = 0$ this behaviour is disturbed by the oscillation of stress components associated with large shear strains, as expected based on the type of results shown in Section 4. Thus, for $b = 0$ and $\rho = 0$, values of ε_f^b are only shown for $\psi_I < 25.3^\circ$ in Fig. 4b, whereas the onset of localization is shown for bands with an initial angle of inclination as large as $\psi_I \simeq 39^\circ$. An analogous but smaller discrepancy between the ranges is found for $b = 0.5$ and $\rho = 0$. On the other hand, for $\rho = 2/\sigma_y$ and for ρ specified by (2.6) the predicted post-localization behaviour is reasonable, with continuously growing voids until void-sheet fracture occurs.

To illustrate the predictions in more detail, Fig. 5a shows the development of the void volume fraction f^b as a function of the maximum principal logarithmic strain ε^b inside the band, for $\psi_I = 30^\circ$ and $b = 0$. Figure 5b shows the corresponding development of the current angle of inclination ψ of the band, and the angle of rotation θ of a line element inside the band, which was initially parallel to the x^1-axis. Clearly, the oscillatory behaviour of f^b predicted for $\rho = 0$ in the post-localization range is unrealistic. This behaviour follows directly from oscillations of the stress components, leading to variations of $\tilde{\sigma}_k^k/3$ between positive and negative values. On the other hand, the onset of localization is predicted at $\varepsilon^b \simeq 0.36$ for $\rho = 0$, while material rotations inside the band are still quite small ($\theta \simeq 5^\circ$), and long before unrealistic oscillations of stresses and void volume fraction are predicted inside the band. In fact, Fig. 5 shows that the development of f^b and θ predicted for $\rho = 0$ is essentially identical to that predicted for $\rho = 2/\sigma_y$ up to $\varepsilon^b \simeq 1$ and $\theta \simeq 23^\circ$.

In a study of the effect of a sharp yield surface vertex on shear band formation HUTCHINSON and TVERGAARD (1981) also included a few results for a kinematic

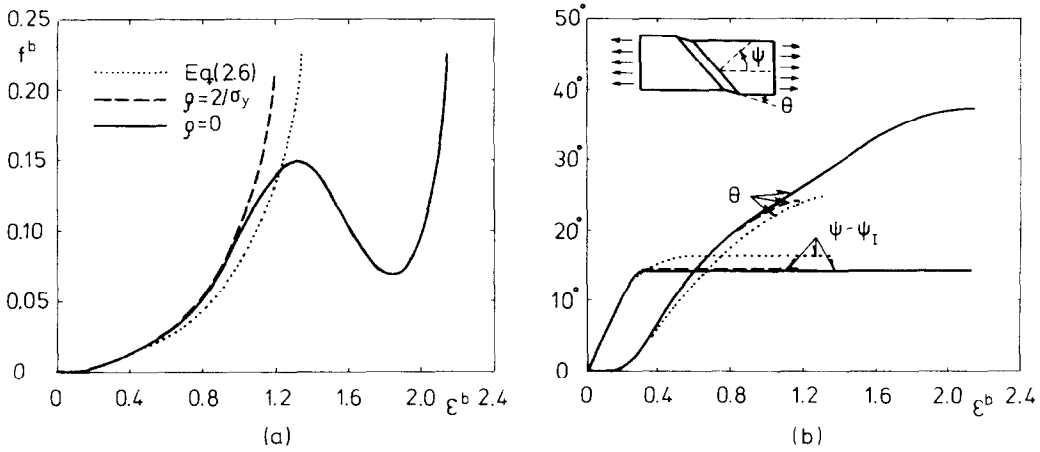

FIG. 5. Uniaxial plane strain tension, $\xi = \kappa = 0$, and strain controlled nucleation, $\Delta f_N = 0.01$, $f_N^0 = 0$, $\varepsilon_N = 0.3$, $s = 0.1$, for $\psi_I = 30^\circ$ and $h = 0$. (a) Void volume fraction vs maximum principal logarithmic strain inside the band. (b) Angles of rotation θ and ψ vs maximum principal logarithmic strain inside the band.

hardening solid, which is in some respects representative of a solid that develops a rounded vertex on the yield surface. It was noted that the value of the angle of rotation θ (see insert in Fig. 5) at the onset of shear localization is small, of the order of 5° or smaller, dependent on the initial inhomogeneity. This agrees with Fig. 5b. Clearly, the rotations are so small that the localization predictions are not affected by whether or not unrealistic stress oscillations are going to occur later, at much larger rotations. The differences between the three curves shown in Fig. 4a for $h = 0$ must be interpreted as a strong sensitivity to very small changes of the constitutive description, induced by assuming different plastic spin constitutive laws. This is supported by the observation in Fig. 2 that the stress increment directions show noticeable variations with the value of ρ. This sensitivity corresponds to earlier findings (RICE, 1976) that localization predictions are strongly affected by small deviations from the assumptions of the classical elastic–plastic solid, in the form of plastic dilation, non-normality of the plastic flow rule, or the formation of a vertex on the yield surface.

Figure 6 shows predictions for exactly the same material description and the same stress and strain state as in Fig. 4, with the only difference that the initial inhomogenity is now ten times smaller, $\Delta f_N = 0.001$. The effect of different ρ-values is analogous to that found in Fig. 4. Thus, in the case of $h = 0$ the minimum localization strain predicted for $\rho = 2/\sigma_y$ is only a little higher than that for $\rho = 0$, whereas the minimum of the curve for ρ according to (2.6) is significantly higher. A difference in the fracture strain predictions of Fig. 6b is that for $h = 0$ and $\rho = 0$ the range of ψ_I-values, in which void-sheet fracture is predicted prior to any unrealistic oscillations of f^b, is relatively smaller than found in Fig. 4b.

In Fig. 7 the solid outside the band is subjected to conditions of axisymmetric uniaxial tension [$\xi = 1$ and $\kappa = 0$ in (5.1)]. The material is here taken to have void nucleation both inside and outside the band, as specified by $f_N^0 = 0.01$ and $\Delta f_N = 0.01$, but all other material parameters are identical to those used above. It is well known

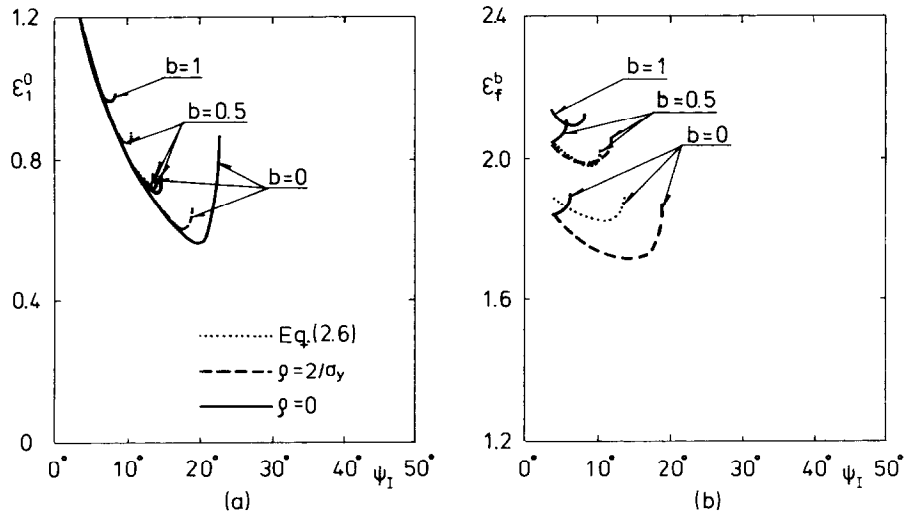

FIG. 6. Uniaxial plane strain tension, $\xi = \kappa = 0$, and strain controlled nucleation, $\Delta f_N = 0.001$, $f_N^0 = 0$, $\varepsilon_N = 0.3$, $s = 0.1$. (a) Localization strain vs initial band orientation. (b) Fracture strain vs initial band orientation.

(NEEDLEMAN and RICE, 1978) that materials subject to axisymmetric straining are far more resistant to localization than under plane strain conditions. Also in Fig. 7a it is seen that the localization strains are much larger than those found in Fig. 4a for the same imperfection amplitude, $\Delta f_N = 0.01$. Regarding the choice of corotational stress rate for $b = 0$, it is also here found that the minimum localization strain for ρ according

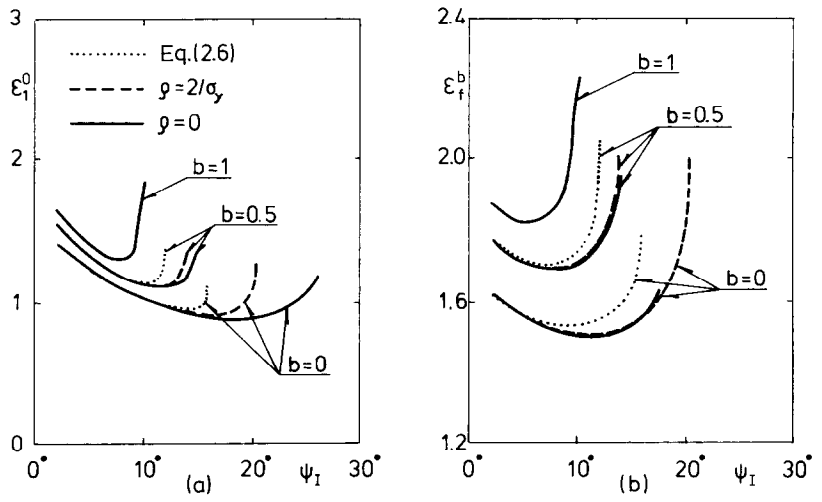

FIG. 7. Uniaxial axisymmetric tension, $\xi = 1$ and $\kappa = 0$, and strain controlled nucleation, $\Delta f_N = f_N^0 = 0.01$, $\varepsilon_N = 0.3$, $s = 0.1$. (a) Localization strain vs initial band orientation. (b) Fracture strain vs initial band orientation.

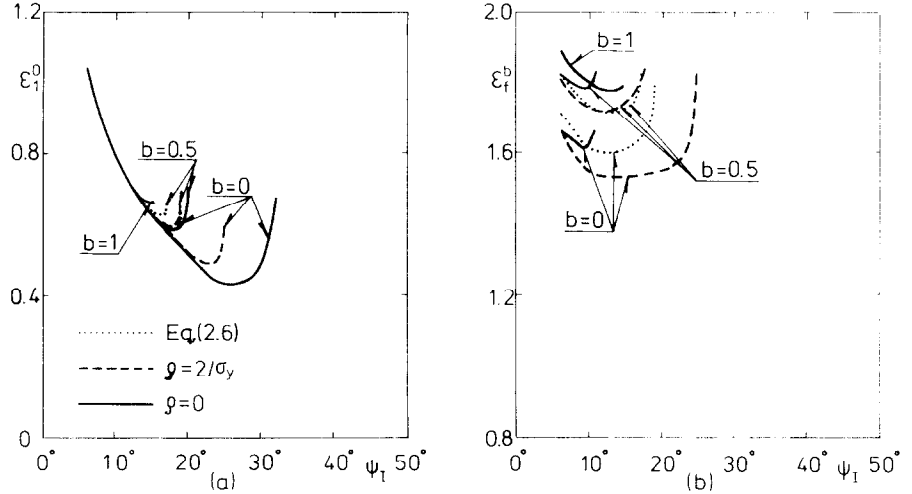

FIG. 8. Uniaxial plane strain tension, $\xi = \kappa = 0$, and strain controlled nucleation, $\Delta f_N = 0$, $f_N^0 = 0.01$, $\varepsilon_N = 0.9$, $s = 0.1$. Inhomogeneity in the initial yield stress, $\sigma_1^b = 0.99\sigma_1^0$. (a) Localization strain vs initial band orientation. (b) Fracture strain vs initial band orientation.

to (2.6) is a little higher than that predicted for $\rho = 2/\sigma_1$, which is again slightly higher than that for $\rho = 0$. However, the difference between these three minima is relatively smaller than found in Figs 4 and 6, which may be related to the fact that the current value of the void volume fraction f^b at the onset of localization is high in Fig. 7a, of the order of 0.06 or higher. It is seen in Fig. 7b, for $b = 0$ and $\rho = 0$, that void-sheet fracture prior to unrealistic oscillations of f^b is predicted within a rather large range of ψ_I-values in this case of axisymmetric uniaxial tension.

The material considered in Fig. 8 is also characterized by strain controlled nucleation, with no initial voids, $f_I^0 = f_I^b = 0$; but here the mean strain for nucleation is taken to be large, $\varepsilon_N = 0.9$, with standard deviation $s = 0.1$, and particle volume fraction $f_N^0 = 0.01$. The inhomogeneity is taken to be represented by a slightly lower initial yield stress inside the band than outside, $\sigma_1^b = 0.99\sigma_1^0$, while $\Delta f_N = 0$ in (5.5). As shown by TVERGAARD (1987), for uniaxial plane strain tension [$\xi = \kappa = 0$ in (5.1)], the kinematic hardening version of this material predicts localization while the void volume fractions are still extremely small, whereas localization predictions for the isotropic hardening material are entirely dependent on the presence of porosity and the softening effect of nucleation. At the minimum localization strain in Fig. 8a, for $b = 0$ and $\rho = 0$, the void volume fractions are $f^b \simeq 10^{-5}$ and $f^0 \simeq 10^{-7}$, so that these predictions are essentially identical to those for a void-free kinematic hardening solid, thus relating to the kinematic hardening localization predictions included in the study of HUTCHINSON and TVERGAARD (1981). It is seen here, for $b = 0$, that the minimum localization strain predicted by taking $\rho = 0$ is relatively more increased by taking $\rho = 2/\sigma_1$ than found in the previous figures. The minimum of the curve for ρ according to (2.6) is actually closer to that for isotropic hardening than to that for $b = 0$ and $\rho = 0$. Thus, also in the absence of porosity, the localization predictions obtained by kinematic hardening are seen to be quite sensitive to the choice of ρ-value, even though

both choices result in realistic material behaviour at large rotations of material elements.

In all cases studied in Figs 4 and 6–8 failure occurs by shear localization, where the final rupture mechanism involves void coalescence in a void-sheet. However, the observation of a void-sheet fracture surface does not guarantee that the onset of localization was caused by porosity (RICE, 1976). Localization may have occurred prior to any void nucleation, e.g. due to the formation of a vertex on the yield surface, and thus the voids leading to the final void-sheet fracture could have nucleated after localization as the strains grow large inside the band. In Fig. 8, for $h = 0$ and $\rho = 0$, the post-localization predictions corresponding to the minimum localization strain become unrealistic due to oscillatory behaviour at large shear strains; but for $\rho = 2/\sigma_y$ the predictions remain quite realistic, representing the mixed effect of the formation of a "rounded vertex" and void nucleation. Thus, for $h = 0$ and $\rho = 2/\sigma_y$ the minimum localization strain ($\psi_l = 23°$) occurs while porosity is still negligible ($f^b \simeq 2 \times 10^{-4}$, $f^0 \simeq 3 \times 10^{-6}$), and void-sheet fracture inside the band is predicted when the strain has reached the level $\varepsilon^b = 1.59$ (see Fig. 8b).

6. DISCUSSION

The investigation of shear band localization in the present paper has shown that the localization behaviour predicted by a kinematic hardening theory is quite sensitive to differences between the corotational stress-rates used for the finite strain generalization of the material model. The differences found in the post-localization regime, where large shear strains occur, were expected based on the differences found in many investigations of kinematic hardening solids subject to simple shear (e.g. see DAFALIAS, 1983, 1985; LORET, 1983). However, the onset of localization occurs prior to large shear strains, where different predictions cannot be explained the same way.

Two of the corotational stress rates considered in the present analyses represent the extreme cases of either neglecting the plastic spin (i.e. the Jaumann rate) or assuming a relatively large plastic part of the spin. The third corotational stress rate considered represents an intermediate case, where just enough plastic spin is assumed to avoid unrealistic stress oscillations at large shear strains. The corresponding three kinematic hardening material models give essentially identical predictions for the development of stress components and other field quantities in the range where the onset of localization is predicted; but still the onset of localization is noticeably delayed by assuming an increased plastic part of the spin. This must be interpreted as a very strong sensitivity of localization predictions to small differences in the constitutive law, analogous to the sensitivity found by RICE (1976) in relation to other constitutive descriptions. It is noted that localization predictions based on a different corotational stress rate, the Green–Naghdi rate, were considered by MEAR and HUTCHINSON (1985), who found rather little difference from predictions based on the Jaumann rate.

The post-localization analyses in the present paper show significant differences between the ductile fracture behaviour predicted by using different finite strain generalizations of kinematic hardening. When plastic spin is neglected, or taken to be a small

part of the total spin, oscillatory stresses are predicted leading to an oscillatory void volume fraction and thus a significant delay of final void-sheet fracture, as shown in Fig. 5. When the effect of plastic spin is increased enough to avoid unrealistic oscillations, this gives rise to a large reduction of the local strain at final fracture, even though the critical overall strain for the onset of localization is slightly increased.

The physical basis for using a stress rate corotational with the elastic spin rather than the total spin (MANDEL, 1971) relates to crystal plasticity. In the crystal, the elastic stress–strain relationship depends on the orientation of the crystal lattice, which is not directly affected by the plasticity resulting from slip on crystal planes (e.g. see ASARO and NEEDLEMAN, 1985), and therefore the stress rates involve corotation with the lattice. In a macroscopic plasticity theory as those considered here the lattice spin is not defined, but is envisioned as the "elastic" or substructure spin, and therefore a constitutive law for the plastic spin can only be a phenomenological approximation that attempts to represent the average behaviour of a polycrystal. It is noted that the plastic spin constitutive law used here is in fact the simplest possible relationship for kinematic hardening (DAFALIAS, 1985; LORET, 1983).

It has been noted that the unconstrained shearing considered in Section 4 is represented in terms of the shear band model by taking $\psi_1 = 45^\circ$ and $\kappa = -1$ in (5.1), and neglecting deformations outside the band. Then, void-sheet fracture could also be analysed in the context of the unconstrained shear model; but this is a case where the value of the porous ductile material model would be limited. In fact, a detailed numerical study of void-sheet fracture in a shear band (TVERGAARD, 1989) has recently shown that sliding contact between the void surface and the inclusion from which the void has nucleated plays an increasing role as the value of the stress ratio κ decays below -0.15, and is certainly very important at $\kappa = -1$.

For biaxially stretched thin sheets it has been emphasized that localization involves no spin, and therefore the influence of kinematic hardening found by TVERGAARD (1978) is unaffected by assumptions regarding the plastic spin. The behaviour is more complex in the range where one of the in-plane principal strains is negative, since here the neck is inclined to the principal axes and spin does take place. However, in this range the localization predictions found by kinematic hardening and isotropic hardening differ so little (e.g. see TVERGAARD, 1987) that other versions of kinematic hardening models are not expected to make much difference.

ACKNOWLEDGEMENT

The work of E.v.d.G. was made possible by a fellowship of the Royal Netherlands Academy of Arts and Sciences.

REFERENCES

ASARO, R. J. and NEEDLEMAN, A. 1985 *Acta Metall.* **33**, 923.
DAFALIAS, Y. F. 1983 *J. appl. Mech.* **50**, 561.
DAFALIAS, Y. F. 1985 *Plasticity Today: Modelling, Methods and Applications* (edited by A. Sawczuk and G. Bianchi), pp. 135–151. Elsevier, London.

GURSON, A. L.	1977a	*J. Engng Materials Technol.* **99,** 2.
GURSON, A. L.	1977b	*Proc. Int. Conf. Fracture* (edited by D. M. R. Taplin), Vol. 2A, pp. 357–364. Pergamon Press, Oxford.
HILL, R.	1952	*J. Mech. Phys. Solids* **1,** 19.
HUTCHINSON, J. W. and TVERGAARD, V.	1981	*Int. J. Solids Struct.* **17,** 451.
LORET, B.	1983	*Mech. Mater.* **2,** 287.
LORET, B.	1985	*Plastic Inst.* (edited by J. Salencon *et al.*), pp. 89–100. Presses Ponts et Chaussées, Paris.
MANDEL, J.	1971	*Plasticite Classique et Viscoplasticite.* Springer, Vienna.
MEAR, M. E. and HUTCHINSON, J. W.	1985	*Mech. Mater.* **4,** 395.
NAGTEGAAL, J. C. and DE JONG, J. E.	1982	*Plasticity of Metals at Finite Strain: Theory Computation and Experiment* (edited by E. H. Lee and R. L. Mallett), pp. 65–102. Stanford.
NEEDLEMAN, A. and RICE, J. R.	1978	*Mechanics of Sheet Metal Forming* (edited by D. P. Koistinen *et al.*), pp. 237–267. Plenum Press, New York.
PAULUN, J. E. and PECHERSKI, R. B.	1987	*Arch. Mech.* (to appear).
RICE, J. R.	1976	*Proc. 14th Int. Congr. Theor. Appl. Mech.* (edited by W. T. Koiter), pp. 207–220. North-Holland, Amsterdam.
RUDNICKI, J. W. and RICE, J. R.	1975	*J. Mech. Phys. Solids* **23,** 371.
STÖREN, S. and RICE, J. R.	1975	*J. Mech. Phys. Solids* **23,** 421.
TVERGAARD, V.	1978	*Int. J. Mech. Sci.* **20,** 651.
TVERGAARD, V.	1981	*Int. J. Fracture* **17,** 389.
TVERGAARD, V.	1982a	*Int. J. Fracture* **18,** 237.
TVERGAARD, V.	1982b	*Int. J. Solids Struct.* **18,** 659.
TVERGAARD, V.	1982c	*J. Mech. Phys. Solids* **30,** 399.
TVERGAARD, V.	1987	*J. Mech. Phys. Solids* **35,** 43.
TVERGAARD, V.	1989	*Int. J. Solids Structures* **25,** 1143.
TVERGAARD, V.	1990a	*Yielding, Damage and Failure of Anisotropic Solids* (edited by J. P. Boehler), pp. 695–709. Mechanical Engineering Publications, London.
TVERGAARD, V.	1990b	*Advances in Appl. Mech.* **27,** 83.
TVERGAARD, V. and NEEDLEMAN, A.	1984	*Acta Metall.* **32,** 157.
VAN DER GIESSEN, E.	1989	*Eur. J. Mech. A/Solids* **8,** 89.
VAN DER GIESSEN, E.	1990	*Yielding, Damage and Failure of Anisotropic Solids* (edited by J. P. Boehler), pp. 187–198. Mechanical Engineering Publications, London.
YAMAMOTO, H.	1978	*Int. J. Fracture* **14,** 347.
ZIEGLER, H.	1959	*Quart. appl. Math.* **17,** 55.